Charge Recombination of Electron−Cation Pairs Formed in Polymer Solids at 20 K through Two-Photon Ionization

Hideo Ohkita, Wataru Sakai, Akira Tsuchida, and Masahide Yamamoto*

Department of Polymer Chemistry, Graduate School of Engineering, Kyoto University, Yoshida, Sakyo, Kyoto 606-01, Japan

Received: June 10, 1997; In Final Form: September 24, 1997[⊗]

The charge recombination at 20 K of a photoejected electron with the parent dopant cation formed in polymer solids through two-photon ionization was examined in terms of long-range electron transfer by electron tunneling. The decay kinetics of isothermal luminescence (ITL) was quantitatively compared with that of the radical cation observed directly by absorption spectroscopy. The comparison showed good agreement for polystyrene but not for poly(alkyl methacrylate)s, which are classified as scission type polymers to high energy radiation. In the latter case, the decrease in radical cations observed at 20 K by absorption measurement was less than that expected from the ITL decay. This disagreement suggests that photoejected electrons in poly(alkyl methacrylate)s are captured in a chemical trap as well as in a physical trap even at 20 K. An electron in a physical trap participates in the charge recombination and emits ITL, but that in a chemical trap does not.

1. Introduction

There have been various investigations on the charge recombination of geminate ion pairs in a condensed phase, which is a primary process following an ionization.[1] In solution systems, the WAS equation[2−5] (an empirical equation) and the square-root law[6] (a first order approximated equation) have been proposed and widely used for the analysis of experimental results. Historically, Onsager derived for the first time the steady-state solution of the Smoluchowski equation for geminate charged particles in a Coulomb potential under the influence of an external field.[7] Currently, a strict solution has been developed for the time-dependent Smoluchowski equation.[6] The decay of ejected electrons in the picosecond order is in agreement with that of the parent radical cation and the decay kinetics obeys the Smoluchowski equation. On the contrary, the decay of ejected electrons in the nanosecond order is inconsistent with that of radical cations owing to the participation of side reactions;[8−10] ejected electrons and radical species produced by irradiation are so reactive that side reactions occur subsequently.

On the other hand, the charge recombination of an ejected electron with the parent cation formed in irradiated solids at a low temperature causes luminescence with an extremely long lifetime. This emission is called isothermal luminescence (ITL) or preglow and the decay kinetics cannot be explained in terms of either the first-order or the second-order kinetics. This ITL intensity $I(t)$ obeys the power kinetics, i.e., the t^{-m} law: $I(t) \propto t^{-m}$, with $m \approx 1$.[11]

There have been proposed mainly two mechanisms for the ITL power decay resulting from the charge recombination of an ejected electron with the parent cation formed in irradiated solids. One is based on the diffusion process of trapped electrons.[12] The long lifetime emission is explained in terms of a small diffusion constant resulting in slow charge recombination rate; the trap depth is much larger than the thermal energy at a low temperature. Debye and Edwards[11] derived theoretically the t^{-m} relationship for the first time in terms of the diffusion mechanism considering a spatial distribution of ejected electrons. However, as Abell and Mozumder[13] pointed out, their model has an inherent weakness in that the initial emission intensity diverges at $t = 0$ just after the irradiation owing to neglect of the normalization of the spatial distribution. Abell and Mozumder reconsidered the Debye-Edwards model using the normalized distribution function and demonstrated the t^{-m} law only on an intermediate time scale; their model also shows the square-root law on a long time scale. After all, the simple diffusion mechanism based on the random walk of trapped electrons results in the square-root law on a long time scale, not in the t^{-m} law. Hamill and Funabashi[14] showed that the t^{-m} behavior can be reproduced over the whole time range using the continuous-time random walk (CTRW) model,[15] by which Scher and Montroll[16] explained the long tail of the transient photocurrent in amorphous solids.

The other mechanism is based on long-range electron transfer by electron tunneling.[17−21] The key assumptions of this mechanism are a spatial distribution of ionic species and the exponential decrease in the rate of electron transfer with increasing distance of electron−cation pairs. It is debatable which mechanism is dominant because there is no conclusive experimental evidence at present. Many authors explained the ITL decay in terms of an electron tunneling model when the ITL decay kinetics is independent of temperature at a low temperature,[22,23] because the hopping rate in the diffusion depends strongly on temperature. Later, Hama et al.[24,25] have proposed a modified equation $I(t) = I_0/(1 + \alpha t)^m$ of the empirical equation[26] $I(t) = I_0/(1 + \alpha t)$ to avoid the divergence of ionic species produced at $t = 0$. They showed that the initial spatial distribution of ejected electrons can be calculated from the Laplace inverse transformation of the modified empirical equation when the value of m is more than unity. If the value of m is less than unity, the distribution function loses its physical meaning because the total amount of ionic species produced diverges into infinity at $t = 0$ just after the irradiation.

Most studies on the ITL have been discussed from the viewpoint of the kinetics of the charge recombination and little attention has been given to chemical reactions. Thus, in an ordinary electron tunneling model, ejected electrons are assumed to be captured in a unique depth trap. However, such an

[⊗] Abstract published in *Advance ACS Abstracts,* November 15, 1997.

S1089-5647(97)01897-X CCC: $14.00

assumption cannot be readily accepted considering the spatially inhomogeneous structure of polymer solids and chemical reactions. Actually, there have been reported many investigations on radiation-induced chemical reactions by ESR measurements.[27−30] For confirmation of this assumption, it is necessary to show a quantitative agreement of the kinetics between the ITL decay and the absorbance decay of ionic species.

In the present study, ionic species were produced through two-photon ionization of a dopant chromophore in polymer solids, not high energy radiation. An intense near-UV light pulse from an excimer laser (351 nm) was used for the selective photoexcitation of the dopant chromophore. The laser pulse is intense enough to feed another photon to the excited chromophore within the lifetime. Consequently, the dopant chromophore is excited to a higher energy level than the ionization potential and then ejects an electron to the polymer matrix. The parent radical cation and the trapped electron in the polymer thus formed are so stable that the color of the parent radical cation can be seen even after a one-year storage from the photoexcitation at room temperature.[31−34]

Herein, we compared the decay kinetics of the ITL with the absorbance of the dopant cation resulting from the charge recombination of electron−cation pairs formed by two-photon ionization of the dopant chromophore.

2. Experimental Section

Chemicals. Polymer samples used here were poly(methyl methacrylate) (PMMA, $M_w = 3.95 \times 10^5$, Scientific Polym. Prod., Inc.), poly(ethyl methacrylate) (PEMA, $M_w = 2.8 \times 10^5$, Scientific Polym. Prod., Inc.), poly(*n*-butyl methacrylate) (PnBMA, $M_w = 10^5$, Wako Pure Chem. Ind., Ltd.), and polystyrene (PSt, $M_w = (1.6-1.8) \times 10^5$, Wako Pure Chem. Ind., Ltd.). All these polymers were purified by reprecipitation from a benzene solution into methanol three times. The glass transition temperatures (T_g) of the polymers are 378 K (PMMA), 339 K (PEMA), 293 K (PnBMA), and 373 K (PSt).[35] The dopant chromophore used here was *N*,*N*,*N*′,*N*′-tetramethylbenzidine (TMB, Wako Pure Chem. Ind., Ltd.), which was purified by recrystallization several times.

Sample Preparation. Sample films for measurements were prepared by the solution cast method. A TMB chromophore was dissolved in a benzene (Dojin Spectrosol) solvent with a polymer powder so as to become ca. 3×10^{-3} mol/L in the final polymer film. The solution was cast on a glass plate in a drybox for 2 days and then was dried by evacuation for 1 day at room temperature. The film was peeled off from the glass plate and was finally dried under vacuum above the T_g until no absorption of the casting solvent was observed with a spectrophotometer. No change in the absorption or emission spectra of the dopant chromophore was observed for the nonphotoirradiated polymer films after the above heating procedure.

Measurements. A sample film was covered with a quartz plate and set tightly on a copper coldfinger of a cryostat (Iwatani Plantech Corp., CRT510). The sample film was, in vacuo, cooled to 20 K and the temperature was kept constant using a PID temperature control unit (Iwatani Plantech Corp., TCU-4). The sample temperature was monitored with a calibrated Au + 0.07% Fe/chromel thermocouple at the sample film position using an indium gasket.

The polymer film doped with TMB was photoirradiated at 20 K by only one 351-nm light pulse from a XeF excimer laser (Lambda Physik, EMG101MSC, ca. 20 ns fwhm and ca. 30 mJ/cm^2). After the prompt fluorescence and phosphorescence of the TMB chromophore disappeared, the emission from the sample film at a fixed temperature of 20 K (this is called ITL or preglow) was measured from 60 s to 25 h after the end of the photoirradiation at 20 K. A photon-counting system was used for the emission intensity measurement, which consists of a photomultiplier (Hamamatsu, R585) and a photon counter (Hamamatsu, C-1230) connected to a personal computer. No ITL was observed in the control experiments where the polymer films without a dopant chromophore were excited by the same procedure.

The steady-state absorption spectra of the photoirradiated sample films were measured in the cryostat with a spectrophotometer (Hitachi, U-3500) using a 2-nm slit width. Ten sheets of sample films prepared freshly, with a total thickness of ca. 2 mm, were put together to gain absorbance of the dopant radical cation high enough to detect. The sample films were photoirradiated at 20 K under the conditions mentioned above. Then we measured the absorption spectra from 3 min to 25 h after the photoirradiation at 20 K. During the intervals of each measurement, the monitor light of the spectrophotometer was shut off to prevent the sample film from being photobleached.

3. Results and Discussion

The kinetics of the geminate recombination by electron tunneling has been theoretically explained by Tachiya and Mozumder.[20] Assuming a proper distribution function of the distance between trapped electrons and solute cations, they demonstrated that the t^{-m} decay profile can be reproduced over a wide time range using an electron tunneling model. On the other hand, Hama et al.[24,25] showed that the Laplace inverse transformation of an empirical ITL decay function (eq 1) enables one to obtain directly the initial distribution function of the distance between a trapped electron and the parent cation. Their model is also essentially based on the geminate recombination by electron tunneling.

$$I(t) = \frac{I_0}{(1 + \alpha t)^m} \tag{1}$$

Here let us summarize the assumptions in the electron tunneling model used by Hama et al.: (i) the charge recombination occurs for geminate pairs; (ii) the recombination reaction proceeds through electron tunneling whose rate constant decreases exponentially with a separation distance r between a trapped electron and the parent cation, $k(r) = \nu \exp(-\beta r)$; (iii) the spatial distribution of ejected electrons is taken into account. The first assumption is valid for our system because the concentration of dopant chromophore is so low (3×10^{-3} mol/L) that each chromophore is considered to be isolated. The second is also reasonable: the above equation holds in most electron transfer reactions. The second and third assumptions are essential to an interpretation of the extremely long lifetime of ITL. In particular, the second assumption enables one to obtain the initial distribution function of the distance between an ejected electron and the parent cation from the Laplace inverse transformation of the ITL decay function. The initial distribution function is connected with the ITL decay through the Laplace inverse transformation, because the electron-transfer rate is expressed in an exponential form that remains similar after a differential operation regarding distance r. The third assumption, a spatial distribution, can be replaced with a trap depth distribution, because the electron-transfer rate is also expressed in an exponential form that remains similar one after a differential operation regarding a trap depth V. We can, therefore, obtain the initial distribution function of trap depth in the same procedure as the spatial distribution function; see Appendix.

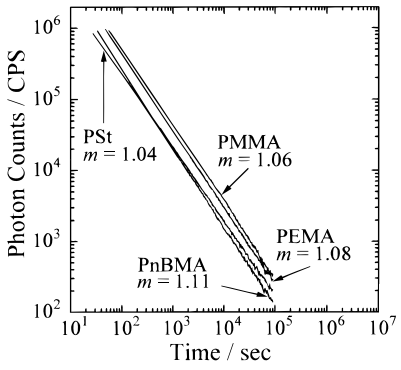

Figure 1. ITL decay of TMB doped in polymer solids photoirradiated at 20 K. The values of *m* represent the slope of the ITL decay; see eq 1.

TABLE 1: Fitting Parameters for ITL Decay of TMB-Doped Polymer Films under One-Shot Irradiation Condition Using Eq 1

	I_0/cps	α/s^{-1}	m
PnBMA	1.3×10^9	23.0	1.11
PEMA	1.9×10^8	2.8	1.08
PMMA	5.0×10^8	7.0	1.06
PSt	1.1×10^7	0.39	1.04

To begin with, we fitted the empirical eq 1 to the observed ITL decay using the least-squares method and obtained the fitting parameters I_0, α, and m. Figure 1 shows the ITL decays of TMB doped in PnBMA, PEMA, PMMA, and PSt after the photoirradiation at 20 K. The fitting parameters are summarized in Table 1. The value of m is uniquely obtained whereas there are many combinations of I_0 and α which can reproduce the observed ITL decay. According to eq 1, the ITL intensity shows a constant value I_0 when the value of αt is negligible in comparison with unity, and it obeys the t^{-m} law when the value of αt is much higher than unity. In other words, the value of α gives the time when the ITL decay starts to obey the t^{-m} law.

The ITL decay deviated from the t^{-m} law was observed over a short time range in radiation chemistry.[24,25] Thus, the deviation gives us information on I_0 and α. On the contrary, such deviation was not observed at all in our system; the ITL decay obeyed the t^{-m} law over the whole time range of measurement. Therefore, the ITL decay in our system has no information on I_0 and α. Although we cannot determine the values of I_0 and α precisely from the fitting, these parameters are not so important in the later discussion.

Next, we measured the absorbance decay of the TMB radical cation ($TMB^{\bullet+}$) from 3 min to 25 h after the photoirradiation at 20 K; the ordinate is normalized with the absorbance at $t =$ 3 min. As shown in Figure 2, the plots of the absorbance of $TMB^{\bullet+}$ in several polymer films vs log t gave an approximately linear relationship. This linear relationship shows that the ITL decay and the decay of $TMB^{\bullet+}$ obey the same kinetics, which can be explained in terms of long-range electron transfer by electron tunneling.[36] Therefore, the discussion on the basis of the distribution function obtained from the Laplace inverse transformation is valuable; the scheme for the charge recombination used by Hama et al. can be also applied to our experimental results.

3.1. Initial Distribution Function of Distance between Photoejected Electron and the Parent Cation. First, we discuss the initial spatial distribution function[37] of the distance between a photoejected electron and the parent cation obtained from the Laplace inverse transformation of the empirical ITL decay function with the fitting parameters. Figure 3 shows the

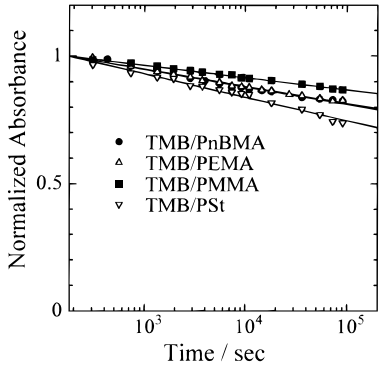

Figure 2. Absorbance decay of $TMB^{\bullet+}$ at 20 K formed through photoionization of the TMB chromophore doped in polymer solids. The ordinate is normalized with the absorbance at $t = 180$ s (3 min after the photoirradiation).

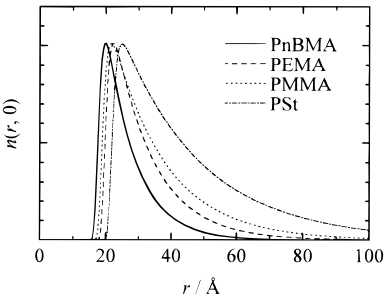

Figure 3. Initial distribution function $n(r, 0)$ of the distance between an ejected electron and the parent cation calculated using eq 2 obtained from the Laplace inverse transformation of the observed ITL decay function fitted to eq 1.

initial distribution functions for TMB/PnBMA, TMB/PEMA, TMB/PMMA and TMB/PSt, respectively. According to Hama et al., when ITL decay can be fitted with the empirical eq 1, the initial distribution function $n(r, 0)$ is given by eq 2 using $k(r) = \nu \exp(-\beta r)$ as the electron-transfer rate:

$$n(r,0)\,\mathrm{d}r = \frac{\beta I_0}{\lambda \alpha^m \Gamma(m)} \nu^{m-1} \exp\left[-(m-1)\beta r - \frac{\nu}{\alpha}\exp(-\beta r)\right] \mathrm{d}r \quad (2)$$

where frequency factor ν and damping factor β are assumed to be 10^9 s^{-1} and 1 Å^{-1},[38] respectively.

Here, we consider how the initial spatial distribution function $n(r, 0)$ depends on the fitting parameters I_0, α, and m. Equation 2 shows that the value of I_0 affects the ordinate of the initial distribution function but not the shape of the initial distribution function. On the contrary, the value of α may influence the shape of the initial distribution function, because the value of α is comparable with that of ν if the ITL decay still obeys the t^{-m} law in a short time range of 10^{-10} s after the photoirradiation. We cannot, therefore, obtain the exact initial distribution function just after the photoirradiation from the observed ITL decay.

Nevertheless, we can partly discuss the initial distribution function obtained from the ITL decay. It should be noticed that the shape of the initial distribution function depends on only the exponential part in eq 2; the preexponential term changes only the ordinate. The first term in the exponential brackets characterizes the decay profile of the initial distribution function. On the other hand, the second term characterizes the rising profile of the initial distribution function. Thus, we can discuss the decay part of the initial distribution function, which is dependent upon the value of m, although we cannot discuss the rising part of the initial distribution function.

The initial distribution obtained from the Laplace inverse transformation of the ITL decay function shows that TMB/PSt system has the most long-range distribution. Trap depth is assumed to be unique for all the polymer matrixes used here. However, polystyrene is expected to have a shallower trap than poly(alkyl methacrylate)s having an ester side-chain whose electron affinity is higher than that of the phenyl group. Considering the difference in trap depth between them, TMB/PSt system has a much more long-range distribution.

Comparing the distribution of trapped electrons among poly(alkyl methacrylate)s, photoejected electrons are farther distributed in the following order: PnBMA < PEMA < PMMA. According to the Wigner-Seitz model, which was applied to the study of the stability criterion for the localization of an excess electron in a nonpolar fluid,[39] trap binding energy V_0 is expressed as a function of the density of solids; its absolute value $|V_0|$ decreases with an increase in the density of solids. Scattering cross section σ increases with the absolute value of trap binding energy $|V_0|$.[40] Since PMMA has the highest density among poly(alkyl methacrylate)s used here, that is, has the smallest $|V_0|$, TMB/PMMA system has the smallest scattering cross section σ. Therefore, if photoejection in our solid system can be interpreted in terms of discussion on the behavior of excess electrons in nonpolar liquids, the difference in the initial distribution may be explained in terms of the difference in the trap binding energy V_0. In Figure 3, the difference in the trap binding energy V_0 is disregarded but, if it was taken into account, polymers with higher density would have much farther distribution of trapped electrons; the difference in the distribution of trapped electrons among poly(alkyl methacrylate)s would be larger.

Next, our attention is focused on the change in the spatial distribution function $n(r, t)$ with time t. In the present experiment, the concentration of dopant chromophore is so dilute that the charge recombination of a photoejected electron with the parent cation can be considered to be a geminate recombination. The geminate recombination obeys the first-order kinetics with the assumption that the one-step electron-transfer process is dominant compared with the electron detrap-retrap processes. Thus the spatial distribution function $n(r, t)$ at time t is given by

$$n(r,t)\,\mathrm{d}r = n(r,0)\exp[-k(r)t]\,\mathrm{d}r = \frac{\beta I_0}{\lambda\alpha^m\Gamma(m)}\nu^{m-1}\exp\left[-(m-1)\beta r - \frac{\nu}{\alpha}\exp(-\beta r)(1+\alpha t)\right]\mathrm{d}r \quad (3)$$

According to eq 3, the shape of the distribution function is independent of the value of α when the observation time t is much higher than the inverse of α. Since the inverse of α corresponds to the time when the t^{-m} law starts to hold; the ITL decay obeyed the t^{-m} law over the time range measured from 10^2 to 10^5 s, therefore, the inverse of α is at least more than of the order of 10^2 s. Thus, it is safe to say that the shape of the distribution function for observation time scale is mainly dependent upon the value of m. We can, therefore, discuss the distribution function within the observed time range even if the values of I_0 and α cannot be determined.

Although the shape of the distribution function within the observed time range is, as described above, mainly characterized by the value of m, it also depends on the values of ν and β. These parameters are not observed values but assumed ones. Thus, we will consider how the values of ν and β affect the shape of the distribution function.

TABLE 2: Percentage of the Decrease in $TMB^{\bullet+}$ Doped in Polymer Solids over the Time Range from 3 min to 25 h after the Photoirradiation at 20 K

	ITL/%[a]	Abs/%[b]	difference/%
PnBMA	48.2	19.6	28.6
PEMA	38.4	18.7	19.7
PMMA	28.9	13.2	15.7
PSt	23.9	23.1	0.8

[a] Calculated from the distribution function of the distance between an ejected electron and the parent cation obtained from the Laplace inverse transformation of the observed ITL decay function fitted to eq 1. [b] Obtained from the fitting curve using eq 4 to the absorption measurement of $TMB^{\bullet+}$ decay at 20 K.

Multiplication of ν by $e^{\beta a}$ makes the distribution function $n(r, t)$ moved parallel in the direction of the r-axis by a. Namely, this procedure is equivalent to the variable transformation of r into $r - a$. Thus, there is no change in the shape of the distribution function with time t because such a procedure leads to not only the shift of the distribution function along the r-axis but also the change in the electron-transfer rate $k(r)$ multiplied by $e^{\beta a}$. Therefore, the percentage of the decrease in a dopant cation within a certain time range is independent of the value of ν.

The replacement of β with βb is equivalent to the variable transformation of r into br leading to the expansion or contraction of the r-axis. Consequently, it is reasonable to conclude that the percentage of the decrease in a dopant cation within a certain time range is also independent of the value of β, that is, the exact values of ν and β are not necessary when we discuss the percentage of the decrease in a dopant cation within a certain time range.

Finally, we compared the fraction of the decrease in radical cations evaluated from the ITL decay using the electron tunneling model with that directly observed by the absorption spectroscopy. The changes in the distribution function $n(r, t)$ with time t shown in Figures 4 are calculated from eq 3. The figures represent the disappearance of electron−cation pairs from 3 min to 25 h after the photoirradiation.

On the other hand, when the ITL decay is expressed by eq 1, the absorbance decay Abs(t) is given by[36]

$$\mathrm{Abs}(t) = \mathrm{Abs}_0 - \mathrm{Abs}_\infty^{\mathrm{dis}}\left[1 - \frac{1}{(1+\alpha t)^{m-1}}\right] \quad (4)$$

where Abs_0 is the absorbance of $TMB^{\bullet+}$ at $t = 0$ and $\mathrm{Abs}_\infty^{\mathrm{dis}}$ is the absorbance corresponding to the disappearance of $TMB^{\bullet+}$ between $t = 0$ and $t = \infty$. Using eq 4, we estimated the percentage of the disappearance from 3 min to 25 h when the amount of radical cations at 3 min is defined as 100 percent.

The second column in Table 2 is the percentage of the disappearance of electron−cation pairs from 3 min to 25 h calculated from the distribution function. The third column is the percentage of the disappearance of the parent cation from 3 min to 25 h directly obtained from the measurement of the absorbance decay of $TMB^{\bullet+}$.

The calculated value in the second column and the observed one in the third column show good agreement for polystyrene whereas they exhibit disagreement for poly(alkyl methacrylate)s. In the latter case, the decrease in radical cations was less than that expected from the ITL decay. This disagreement suggests that some photoejected electrons are captured in a deeper trap and cannot recombine with the parent cation at 20 K; there is another deep trap besides a shallow trap in photoirradiated poly(alkyl methacrylate)s even at 20 K.

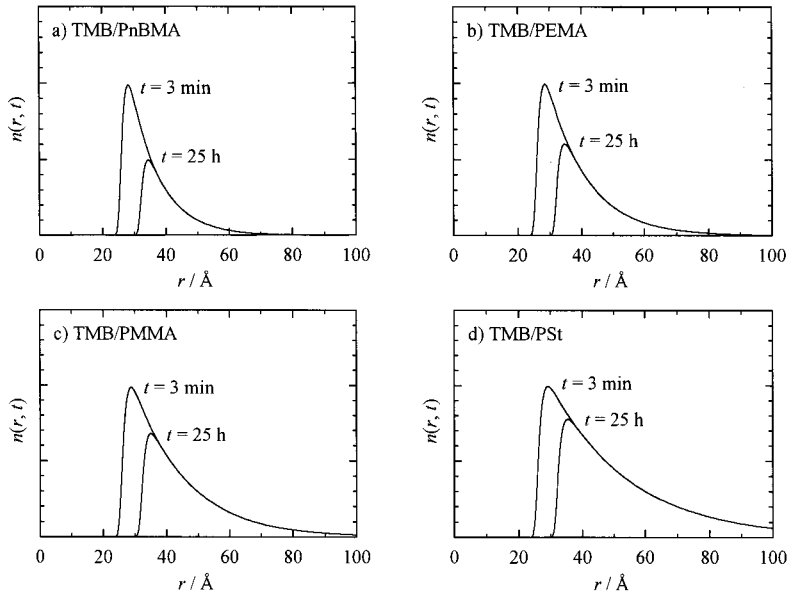

Figure 4. Distribution function $n(r, t)$ of the distance between an ejected electron and the parent cation calculated using eq 3 obtained from the Laplace inverse transformation of the observed ITL decay function fitted to eq 1. The distribution functions $n(r, t)$ at 3 min and 25 h after the photoirradiation at 20 K.

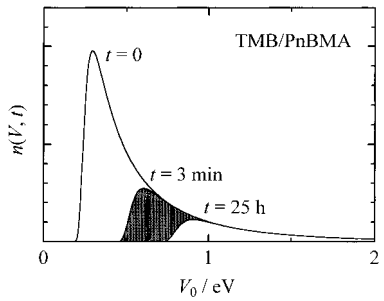

Figure 5. Distribution function of a trap depth (eq 13) calculated from the Laplace inverse transformation of the observed ITL decay function fitted to eq 1. The shaded portion in the figure represents the decrease in the $TMB^{\bullet+}$ due to the charge recombination over the time range from 3 min to 25 h after the photoirradiation at 20 K. The parameters used are as follows: $I_0 = 1.3 \times 10^9$ cps, $\alpha = 23.0$ s^{-1}, $m = 1.11$, $\nu = 10^9$ s^{-1}, and $r_{DA} = 35$ Å.

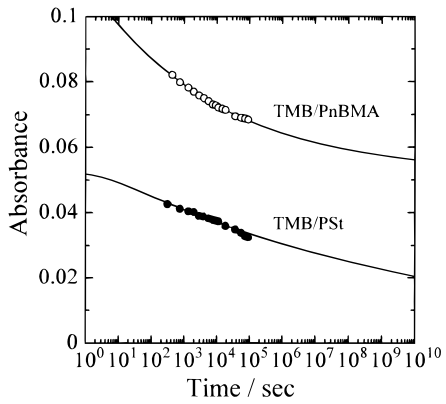

Figure 6. Absorbance decay of $TMB^{\bullet+}$ for TMB/PnBMA and TMB/PSt at 20 K. The solid lines are the fitting curve using eq 4 with the same parameters obtained from the ITL decay fitting: $\alpha = 23.0$, $m = 1.11$ for TMB/PnBMA; $\alpha = 23.0$, $m = 1.11$ for TMB/PSt. The fitting parameters for the absorbance decay are as follows: $Abs_0 = 0.135 > Abs_\infty^{dis} = 0.0838$ for PnBMA; $Abs_0 = 0.0526 \approx Abs_\infty^{dis} = 0.0548$ for PSt.

3.2. Initial Distribution Function of Trap Depth. As an example, we obtained the initial trap-depth distribution function $n(V, 0)$ of TMB/PnBMA from the Laplace inverse transformation of the ITL decay function; see eq 13. The parameters used here were as follows: $I_0 = 1.3 \times 10^9$ cps, $\alpha = 23.0$ s^{-1}, $m = 1.11$, $\nu = 10^9$ s^{-1}, and $r_{DA} = 35$ Å.

As shown in Figure 5, the explanation of the t^{-m} behavior over the wide time range requires a wide trap-depth distribution from 0.5 to 2.0 eV. An explanation can be made from the viewpoint of the very narrow spectral distribution of excitation laser pulses if we disregard the spatial distribution of electron−cation pairs.[41] However, the wide trap-depth distribution contradicts the temperature independence of the ITL decay kinetics. Besides, the decrease in ionic species calculated from the initial trap-depth distribution is too large compared with that obtained from the absorbance measurement given above; the former is about 50% whereas the latter is about 20%. Therefore, we cannot adopt the trap-depth distribution model without a spatial distribution.

3.3. Spatial Distribution of Photoejected Electrons in Shallow Trap and Deep Trap. In subsection 3.1, we considered only a spatial distribution of photoejected electrons and disregarded the trap-depth distribution. Here, to explain the difference between the ITL decay and the absorbance decay, we take account of another trap that is so deep that the trapped electron cannot participate in the charge recombination with the parent cation. In other words, we assumed that the ITL results from the charge recombination from a shallow trap and the absorbance is the sum of the shallow trap and deep trap not participating in the charge recombination.

The absorbance decay of $TMB^{\bullet+}$ indicates the existence of a deep trap not participating in the charge recombination. Figure 6 shows the results for the fitting of eq 4 to the absorbance of $TMB^{\bullet+}$ in PnBMA and PSt as an example. The value of Abs_0 is higher than that of Abs_∞^{dis} for poly(alkyl methacrylate)s, while the value of Abs_∞^{dis} is almost equal to that of Abs_0 for polystyrene. A part of $TMB^{\bullet+}$ in poly(alkyl methacrylate) solids remains even at $t = \infty$. This finding also indicates the existence of a deep trap not participating in the charge recombination.

In Figure 7, the fraction of shallow trap (recombined) was that of the absorbance decay of $TMB^{\bullet+}$ from 3 min to 25 h after the photoirradiation when the absorbance at 3 min was defined as 100%. The fraction of shallow trap (remaining) was calculated from the ratio of the disappearance to the remaining of distribution function obtained from the Laplace inverse

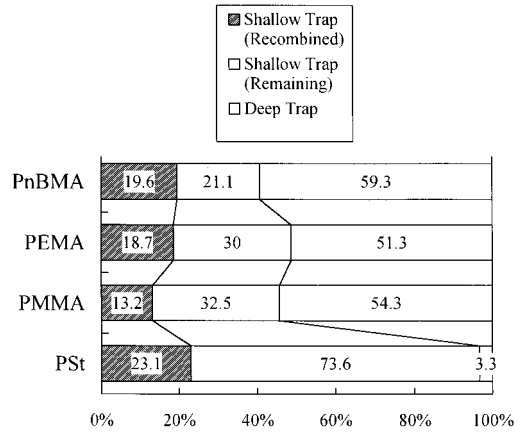

Figure 7. Bar charts for the percentage of shallow and deep traps. Photoejected electrons captured in a shallow trap recombine with the parent cation at 20 K. However, photoejected electrons in a deep trap stay in the trap and cannot recombine with the parent cation at 20 K.

transformation of the ITL decay during the same time domain. Then, the fraction of deep trap was estimated from the subtracting both of the above from 100%. As shown in Figure 7, the ratio of the shallow and deep traps is about 40:60−50:50 for poly(alkyl methacrylate)s used here. This suggests that 50−60% of photoejected electrons are captured in deep trap sites for poly(alkyl methacrylate)s. This estimation is very rough, but suggests that deep trap as well as shallow traps exists even at 20 K where major motions of the polymer chain are frozen.

In irradiated polymer solids, charged species produced by radiation was reported to cause side-chain elimination, main-chain scission, and cross-linking.[42] In poly(alkyl methacrylate) solids, a main-chain scission is reported to be induced by photoionization of the dopant chromophore[29,30] as well as radiation.[27,28] On the other hand, polystyrene is more highly resistant to radiation than poly(alkyl methacrylate)s, although it is classified as a cross-linking type.[42,43] Thus, the disagreement in poly(alkyl methacrylate)s might be related to the photoinduced chemical reaction. However, a large scale chemical reaction might be impossible at a temperature as low as 20 K, because only small species such as electrons, protons, and methyl group can migrate and transfer at 20 K. One possible explanation is that the shallow trap is a physical trap, e.g., a small cavity of polymer matrix, and the deep trap is a chemical trap, e.g., ester anion radical,[29,30,44,45] which is a precursor of main-chain scission.

4. Conclusion

On the basis of an electron tunneling model, the initial distribution function of the distance between a photoejected electron and the parent cation was calculated from the Laplace inverse transformation of the observed ITL decay function. The decrease in ionic species estimated from the initial distribution was found to be consistent with that from the absorbance measurement of the dopant cation for polystyrene but not for poly(alkyl methacrylate)s. In the case of poly(alkyl methacrylate)s, some photoejected electrons are captured in a deep trap site and change into a precursor of chemical reaction, e.g., ester anion radical, even at 20 K where major motion of the polymer chain is frozen.

Acknowledgment. We express our sincere thanks to Professor Yoshimasa Hama of Waseda University for helpful discussions. This work was supported by a Grant-in-Aid on Primary-Area-Research "Photoreaction Dynamics" (No. 06239107) from the Ministry of Education, Science, Sports and Culture of Japan.

Appendix

The following kinetics equation holds for the geminate charge recombination:

$$\frac{\mathrm{d}}{\mathrm{d}t}n(r,V,t)\,\mathrm{d}r\,\mathrm{d}V = -k(r,V)n(r,V,t)\,\mathrm{d}r\,\mathrm{d}V$$
$$n(r,V,t)\,\mathrm{d}r\,\mathrm{d}V = n(r,V,0)\exp[-k(r,V)t]\,\mathrm{d}r\,\mathrm{d}V \tag{5}$$

where $n(r, V, t)\,\mathrm{d}r\,\mathrm{d}V$ is the number of electron−cation pairs as a function of the distance between the electron−cation pairs r, trap depth V, and time t from just after the formation of initial electron−cation pairs, and $k(r, V)$ is the rate of electron transfer.

Assuming that the trap-depth distribution is independent of the spatial distribution, $n(r, V, t)$ can be divided into the product of $n(r, t)$ and $n(V, t)$,

$$n(r,V,t) = n(r,t)n(V,t) \tag{6}$$

Thus, we obtain the following equation with apparent quantum efficiency of emission λ,

$$I(t) = -\lambda\frac{\mathrm{d}}{\mathrm{d}t}\int\int n(r,V,t)\,\mathrm{d}r\,\mathrm{d}V$$
$$= -\lambda\int\int\frac{\mathrm{d}}{\mathrm{d}t}n(r,V,t)\,\mathrm{d}r\,\mathrm{d}V \tag{7}$$
$$= \lambda\int\int k(r,V)n(r,0)n(V,0)\exp[-k(r,V)t]\,\mathrm{d}r\,\mathrm{d}V$$

Here, we disregard the spatial distribution: the following delta function is introduced for the spatial distribution,

$$n(r,0) = n\delta(r - r_{\mathrm{DA}}) \tag{8}$$

then the ITL intensity $I(t)$ is

$$I(t) = \lambda n\int k(r_{\mathrm{DA}},V)n(V,0)\exp[-k(r_{\mathrm{DA}},V)t]\,\mathrm{d}V$$
$$= \lambda n\int k(V)n(V,0)\exp[-k(V)t]\,\mathrm{d}V \tag{9}$$

where $k(V)$ is given by the WKB approximation;

$$k(V) = k(r_{\mathrm{DA}},V) = \nu\exp\left(-\frac{2\sqrt{2m_{\mathrm{e}}(V-E)}}{\hbar}r_{\mathrm{DA}}\right) \tag{10}$$

Then we carried out the following variable transformation from V into $k(V)$;

$$k(V)\,\mathrm{d}V = -\frac{\hbar}{r_{\mathrm{DA}}\sqrt{2m_{\mathrm{e}}}}\sqrt{V-E}\,\mathrm{d}k(V) \tag{11}$$

Finally, the ITL intensity can be expressed by

$$I(t) = -\lambda n\int_{\nu}^{0} n(V,0)\exp[-k(V)t]\frac{\hbar}{r_{\mathrm{DA}}}\sqrt{\frac{V-E}{2m_{\mathrm{e}}}}\,\mathrm{d}k(V)$$
$$= \frac{\lambda n\hbar}{r_{\mathrm{DA}}\sqrt{2m_{\mathrm{e}}}}\int_{0}^{\infty} n(V,0)\sqrt{V-E}\exp[-k(V)t]\,\mathrm{d}k(V) \tag{12}$$

Because this equation is satisfied with the Laplace transformation, the initial trap-depth distribution $n(V, 0)$ can be obtained from the Laplace inverse transformation of the ITL intensity

function $I(t)$,

$$n(V,0)\sqrt{V-E} = \frac{r_{DA}\sqrt{2m_e}}{\lambda n\hbar}L^{-1}[I(t)]$$

$$n(V,0) = \frac{r_{DA}\sqrt{2m_e}}{\lambda n\hbar}\frac{1}{\sqrt{V-E}}L^{-1}\left[\frac{I_0}{(1+\alpha t)^m}\right] \qquad (13)$$

$$= \frac{r_{DA}\beta I_0 \nu^{m-1}}{n\hbar\lambda\alpha^m\Gamma(m)}\sqrt{\frac{2m_e}{V-E}} \times \exp\left[-(m-1)\beta r_{DA} - \frac{\nu}{\alpha}\exp(-\beta r_{DA})\right]$$

where β is given by the following equation:

$$\beta = \frac{2\sqrt{2m_e(V-E)}}{\hbar} = \frac{2\sqrt{2m_eV_0}}{\hbar} \qquad (14)$$

References and Notes

(1) Warman, J. M. In *The Study of Fast Processes and Transient Species by Electron Pulse Radiolysis*; Baxendale, J. H.; Busi, F., Eds.; Reidel: Dordrecht, 1982.

(2) Warman, J. M.; Asmus, K.-D.; Schuler, R. H. *J. Phys. Chem.* **1969**, *73*, 931.

(3) Warman, J. M.; Rzad, S. J. *J. Chem. Phys.* **1970**, *52*, 485.

(4) Rzad, S. J.; Infelta, P. P.; Warman, J. M.; Schuler, R. H. *J. Chem. Phys.* **1970**, *52*, 3971.

(5) Tachiya, M. *J. Chem. Phys.* **1979**, *70*, 4701.

(6) Hong, K. M.; Noolandi, J. *J. Chem. Phys.* **1978**, *68*, 5163.

(7) Onsager, L. *Phys. Rev.* **1938**, *54*, 554.

(8) Yoshida, Y.; Tagawa, S.; Tabata, Y. *Radiat. Phys. Chem.* **1986**, *28*, 201.

(9) Yoshida, Y.; Tagawa, S.; Washio, M.; Kobayashi, H.; Tabata, Y. *Radiat. Phys. Chem.* **1989**, *34*, 493.

(10) Yoshida, Y.; Tagawa, S. In *Dynamics and Mechanisms of Photo-induced Electron Transfer and Related Phenomena*; Mataga, N.; Okada, T.; Masuhara, H., Eds.; Elsevier: Amsterdam, 1992.

(11) Debye, P.; Edwards, J. O. *J. Chem. Phys.* **1952**, *20*, 236.

(12) In the present paper, we define the term "a trapped electron" as an electron captured in the matrix; including trapped electrons, solvated electrons, radical anions, and other anionic species.

(13) Abell, G. C.; Mozumder, A. *J. Chem. Phys.* **1972**, *56*, 4079.

(14) Hamill, W. H.; Funabashi, K. *Phys. Rev. B* **1977**, *16*, 5523.

(15) Montroll, E. W.; Weiss, G. H. *J. Math. Phys.* **1965**, *6*, 167.

(16) Scher, H.; Montroll, E. W. *Phys. Rev. B* **1975**, *12*, 2455.

(17) Mikhailov, A. I. *Dokl. Akad. Nauk SSSR* **1970**, *197*, 136.

(18) Tachiya, M.; Mozumder, A. *Chem. Phys. Lett.* **1974**, *28*, 87.

(19) Dainton, F. S.; Pilling, M. J.; Rice, S. A. *J. Chem. Soc., Faraday Trans. 2* **1975**, *71*, 1311.

(20) Tachiya, M.; Mozumder, A. *Chem. Phys. Lett.* **1975**, *34*, 77.

(21) Pilling, M. J.; Rice, S. A. *J. Phys. Chem.* **1975**, *79*, 3035.

(22) Kieffer, F.; Meyer, C.; Rigaut, J. *Chem. Phys. Lett.* **1971**, *11*, 359.

(23) Kieffer, F.; Meyer, C.; Rigaut, J. *Int. J. Radiat. Phys. Chem.* **1974**, *6*, 79.

(24) Hama, Y.; Kimura, Y.; Tsumura, H.; Omi, N. *Chem. Phys.* **1980**, *53*, 115.

(25) Hama, Y.; Gouda, K. *Radiat. Phys. Chem.* **1983**, *21*, 185.

(26) Bagdasar'yan, Kh. S.; Milyutinskaya, R. I.; Kovalev, Yu. V. *Khim. Vysok. Energ.* **1967**, *1*, 127.

(27) Tanaka, M.; Yoshida, H.; Ichikawa, T. *Polym. J.* **1990**, *22*, 835.

(28) Yoshida, H.; Ichikawa, T. In *Recent Trends in Radiation Polymer Chemistry*; Okamura, S., Ed.; Advances in Polymer Science 105; Springer-Verlag: Berlin, 1993.

(29) Sakai, W.; Tsuchida, A.; Yamamoto, M.; Matsuyama, T.; Yamaoka, H.; Yamauchi, J. *Macromol. Rapid Commun.* **1994**, *15*, 551.

(30) Sakai, W.; Tsuchida, A.; Yamamoto, M.; Yamauchi, J. *J. Polym. Sci., Polym. Chem. Ed.* **1995**, *33*, 1969.

(31) Tsuchida, A.; Nakano, M.; Yoshida, M.; Yamamoto, M.; Wada, Y. *Polym. Bull.* **1988**, *20*, 297.

(32) Yamamoto, M.; Tsuchida, A.; Nakano, M. *MRS Int. Meeting Adv. Mater.* **1989**, *12*, 243.

(33) Tsuchida, A.; Sakai, W.; Nakano, M.; Yoshida, M.; Yamamoto, M. *Chem. Phys. Lett.* **1992**, *188*, 254.

(34) Tsuchida, A.; Sakai, W.; Nakano, M.; Yamamoto, M. *J. Phys. Chem.* **1992**, *96*, 8855.

(35) Peyser, P. In *Polymer Handbook*, 3rd ed.; Brandrup, J.; Immergut, E. H., Eds.; John Wiley & Sons: New York, 1989.

(36) Ohkita, H.; Sakai, W.; Tsuchida, A.; Yamamoto, M. *Bull. Chem. Soc. Jpn.*, in press.

(37) Correctly speaking, the initial distribution function $f(r)$ represents the probability density that an ejected electron exists at a distance r from the parent cation. Thus, the number of ejected electrons between r and $r + dr$ is proportional to $f(r)4\pi r^2\,dr$ in the three dimensions. The relationship between $f(r)$ and $n(r, 0)$ is given by $n(r, 0)\,dr \propto f(r)4\pi r^2\,dr$. In the present paper, for the sake of convenience, $n(r, 0)$ is also called initial distribution function.

(38) According to the WKB approximation, the value of β can be expressed by eq 14. Thus, the value of β is estimated to be ca. 1 $Å^{-1}$ using eq 14 with the assumption that the binding energy for trapped electrons $V - E$ ($= V_0$) is about 1 eV.

(39) Springett, B. E.; Jortner, J.; Cohen, M. H. *J. Chem. Phys.* **1968**, *48*, 2720.

(40) Basak, S.; Cohen, M. H. *Phys. Rev. B* **1979**, *20*, 3404.

(41) Miyasaka, H.; Mataga, N. *Chem. Phys. Lett.* **1987**, *134*, 480.

(42) Schnabel, W. *Polymer Degradation—Principles and Practical Applications*; Carl Hanser Verlag: Munich, 1982.

(43) O'Donnell, J. H.; Pomery, P. J. *J. Polym. Sci., Polym. Symp.* **1976**, *55*, 269.

(44) Torikai, A.; Kato, H.; Kuri, Z. *J. Polym. Sci., Polym. Chem. Ed.* **1976**, *14*, 1065.

(45) Torikai, A.; Okamoto, S. *J. Polym. Sci., Polym. Chem. Ed.* **1978**, *16*, 2689.